JOURNAL OF THERMOPHYSICS AND HEAT TRANSFER
Vol. 16, No. 3, July–September 2002

Approach for Calculating Thermophysical Properties with the Help of Statistical Thermodynamics

Jurij Avsec* and Milan Marčič†
University of Maribor, SI-2000 Maribor, Slovenia

In engineering practice, refrigeration and cryogenics are processes of vital importance. To design devices for this field, it is necessary to be familiar with the thermodynamic properties of state in a one-phase and a two-phase environment. In most cases, thermodynamic tables and diagrams are used, as well as different empirical functions obtained from measurements. In our case, quantum statistical thermodynamics were used to calculate thermodynamic properties of state. The mathematical model for calculation of the thermodynamic properties of state in real-gas, one-component systems is treated. The virial expansion theory with quantum corrections was used to calculate the thermodynamic functions of state. The mathematical model of a weakly coupled, highly degenerate quantum fluid is also dealt with. We have calculated the thermodynamic properties of state with the help of the quantum field theory for many particle systems using finite temperature formalism. We used the Feynman–Dyson perturbation theory. We developed the expression for the grand potential of normal Maxwell–Boltzmann systems with the help of Green function temperatures and Feynman's diagrams. The results of the analysis were compared with experimental data, and they show good agreement.

Nomenclature

A	=	free energy, J/kmol
A_i	=	coefficients
b_1, b_2, b_3	=	cluster coefficients, m^{-3}
C	=	coefficient
C_p	=	specific heat capacity at constant pressure per mole, J/kmol · K
C_v	=	specific heat capacity at constant volume per mole, J/kmol · K
c_0	=	velocity of sound, m/s
c_1, c_2, c_3	=	constants
c^+, c^-	=	creation and annihilation operators
D	=	diameter of hard core of molecule, m
E	=	energy, J
E_k	=	complete set of single-particle quantum numbers
e_k	=	energy of molecule, J
f	=	number of degrees of freedom
G	=	Green function
G_t	=	coefficient for three-molecule cluster integral
H	=	enthalpy, J/kmol
H_H	=	Hamiltonian, J
H_t	=	coefficient for three-molecule cluster integral
h	=	Planck constant, J · s
$\hbar = h/(2\pi)$	=	Planck constant, J · s
I_t	=	quantum correction coefficient for three-molecule cluster integral
i	=	imaginary number
k	=	momentum, kg · m/s
k_B	=	Boltzmann constant, J/K
M	=	molecular mass, kg/kmol
m	=	mass, kg
N	=	number of molecules in system
n_k	=	molecular distribution
P	=	coefficient, 1/J
p	=	momentum, kg · m/s
p_p	=	pressure, Pa
q	=	momentum, kg · m/s
q_c	=	charge, As
R_m	=	universal gas constant, J/kmol · K
r	=	intermolecular distance, m
S	=	entropy, J/kmol · K
s_p	=	molecular spin
T	=	temperature, K
T_k	=	kinetic energy, J
T_{k1}	=	single-particle operator of kinetic energy
T^*	=	reduced temperature
U	=	internal energy, J/kmol
V	=	molar volume, m^3/kmol
V_p	=	interpaticle potential energy, J
x_k	=	space coordinate of particle k, m
y	=	reduced Lennard–Jones function
z	=	activity
β	=	Boltzmann factor, 1/J
Γ	=	gamma function
ε	=	Lennard–Jones parameter, J
ζ	=	integration variable
η	=	integration variable
η_c	=	convergence time, s
$\vartheta_1, \vartheta_2, \vartheta_3$	=	angles of triangle, rad
λ	=	integrational variable
λ_{LJ}	=	Lennard–Jones coefficient, J · m^{12}
λ_T	=	thermal wavelength, m
μ	=	chemical potential, J
ν	=	three-body coefficient
ρ	=	density, kg · m^{-3}
Σ	=	self-energy, J
Σ^*	=	proper self-energy, J
σ	=	Lennard–Jones parameter, m
τ	=	time, s
$\varphi(x)$	=	dimensionless function
ψ	=	wave function
$\hat{\psi}$	=	field operator
Ω	=	thermodynamic potential, J/kmol
Ω_R	=	influence of ring diagrams to the thermodynamic potential, J/kmol

Presented as Paper 2000-2509 at the AIAA 34th Thermophysics Conference, Denver, CO, 19–22 June 2000; received 4 October 2000; revision received 7 March 2002; accepted for publication 12 March 2002.

*Assistant Professor and Mechanical Engineer, Department of Thermodynamics, Faculty of Mechanical Engineering, P.O. Box 224, Smetanova ul. 17. Member AIAA.

†Professor, Department of Thermodynamics, Faculty of Mechanical Engineering, P.O. Box 224, Smetanova ul. 17.

ω_n = discrete variable

Subscripts

kin = kinetic energy of N molecules
kin-1 = kinetic energy of individual molecule
pot = potential energy

Introduction

In engineering practice, processes occuring in the liquid–gas region are of vital importance. To design devices for this field of activity, it is necessary to know the thermodynamic properties of state in one- and two-phase environments for pure refrigerants and their mixtures.

For fluids composed of molecules of small mass, with low moments of inertia and low molecular masses, such as He, the classical expressions for the calculation obtained by classical statistical thermodynamics of thermodynamic properties of state do not give very good results at lower temperatures, for example, in the area of the cryogenic processes. There are two kinds of quantum effects that must be considered.[1] For such molecules, the thermal wavelength $\lambda_T = (2\pi\hbar^2/mk_BT)^{1/2}$ will be relatively large, and quantum corrections must be taken into account. These phenomena are called diffraction effects and become important when the thermal wavelength is the size of the radius of molecules. These effects are linked to the wave nature of molecules and are a direct consequence of Heisenberg's uncertainty principle. The effects of statistics become important when the thermal wavelength is the size of the average distance between particles. These effects are associated with exchange or symmetry effects of indistinguishable molecules due to their boson or fermion character. In most cases, for engineering practice, the refrigeration and cryogenic effects of quantum statistics are unimportant. On the other hand, there are practical cases wherein diffraction effects make a significant contribution to thermodynamic properties.[2]

The physical world consists of the interaction of many-particle systems. Let us consider a system of N equal molecules of a real gas or a real liquid. Molecules move either idividually or in small instantaneous clusters. The size and shape of the clusters alter due to the existence of intermolecular and intramolecular interactions between electrons and nuclei in the system.

The energy inherent in such a molecular system consists of 1) the kinetic energy of molecules and atoms, 2) the potential intermolecular energy, 3) the energy of electrons because of the energy level to which they belong, and 4) the energy of nuclei because of the energy level to which they belong.

To obtain an accurate calculation, it would be necessary to solve the Schrödinger equation (see Ref. 3) for several particles:

$$\left(-\sum \frac{h^2}{4\pi^2 m_i}\nabla_i^2 + \frac{1}{2}\sum_i \sum_j \frac{q_i q_j}{r_{ij}^2}\right)\psi = \frac{h}{2\pi i}\frac{\partial \psi}{\partial \tau} \qquad (1)$$

where the sums are taken over all nuclei and electrons with appropriate masses m_i and charges q_i. An accurate description of such systems requires the inclusion of the interparticle potentials in the many-paricle Schrödinger equation. In principle, the N-body wave function in configuration space contains all possible information, but a direct solution of the Schrödinger equation is impractical. It is, therefore, necessary to resort to other techniques, and we used the concept of second quantization. Any solution of such a differential equation is a difficult task, though reasonably accurate results can be obtained by means of some generalizations[3]:

1) Intermolecular forces are much weaker than intramoleular forces, therefore, both intramolecular and intermolecular forces can be treated quite independently.

2) Potential intermolecular energy depends merely on the position of nuclei in space.

3) The effect of the orientation of the molecule in space has been neglected.

4) Each of the modes of motion is independent of the others.

Statistical Thermodynamics

In spite of the aforementioned simplifications, the many-body Schrödinger equation (1) is still mathematically difficult to solve, and so we applied statistical thermodynamics with quantum corrections to compute the thermodynamic functions of state. For this purpose, we applied the grand canonical partition.[4] Considering a single-component gas in V, we assume that the system is in thermodynamic equilibrium with environment characterized by the temperature T and chemical potential μ. A microscopic state may be regarded as a quantum state belonging to an energy eigenvalue E_{jr} with the number of paricles N. In the grand canonical ensemble,[4] we can define thermodynamic potential Ω (Ref. 4):

$$\Omega = -k_BT\,\ell n\left[\sum_{j=1}^{N}\exp(\mu j\beta)\sum_{s=1}^{j}\exp(-E_s\beta)\right] \qquad (2)$$

$$\beta = \frac{1}{k_BT} \qquad (3)$$

Utilizing the semiclassical formulation for the purpose of the grand canonical ensemble, we get

$$\Omega = -k_BT\,\ell n\left[\sum_{j=1}^{N}\exp(\mu j\beta)\frac{1}{j!h^{jf}}\int\cdots\int\exp\left(-\frac{E_{\text{kin}}}{k_BT}\right)\right.$$
$$\left.\times\,d\boldsymbol{k}_1,\ldots,d\boldsymbol{k}_j\int\cdots\int\exp\left(-\frac{E_{\text{pot}}}{k_BT}\right)d\boldsymbol{r}_1,\ldots,d\boldsymbol{r}_j\right] \qquad (4)$$

We can define the coefficient z and cluster coefficients b_1, b_2, and b_3 for Lennard–Jones intermolecular potential:

$$z = \exp(\mu\beta)\frac{1}{h^f}\int\cdots\int\exp\left(-\frac{E_{\text{kin-1}}}{k_BT}\right)d\boldsymbol{k}_1 \qquad (5)$$

Now we can introduce coefficients b_1, b_2, and b_3 into Eq. (4):

$$b_1 = 1, \qquad b_2 = \frac{1}{2!}\int\left[\exp\left(-\frac{V_{p12}}{k_BT}\right)-1\right]d\boldsymbol{r}_2$$

$$b_3 = \frac{1}{3!}\int\int\left[\exp\left(-\frac{V_{p123}}{k_BT}\right)-\exp\left(-\frac{V_{p12}}{k_BT}\right)\right.$$
$$\left.-\exp\left(-\frac{V_{p13}}{k_BT}\right)-\exp\left(-\frac{V_{p23}}{k_BT}\right)+2\right]d\boldsymbol{r}_2\,d\boldsymbol{r}_3 \qquad (6)$$

With the help of Eqs. (4–6) and with the supposition that we keep only dominant terms (zV, z^2V, z^3V, ...) and that all higher terms (z^2V^2, z^3V^2, z^4V^2) are neglected, we can express the thermodynamic potential Ω as

$$\Omega = -Vk_BT\sum_{k=1}^{\infty}b_kz^k \qquad (7)$$

We can calculate cluster coefficients b_2 and b_3 for the Lennard–Jones fluid[1,5]:

$$b_2 = \frac{\pi}{6}\left(4^{\frac{1}{12}}\sigma\right)\left(\frac{\varepsilon}{k_BT}\right)^{\frac{1}{4}}\sum_{t=0}^{\infty}\frac{2^t}{t!}\Gamma\left(\frac{2t-1}{4}\right)\left(\frac{\varepsilon}{k_BT}\right)^{t/2} \qquad (8)$$

$$b_3 = (b_3)_{\nu=0} + \nu\left(\frac{\partial b_3}{\partial \nu}\right)_{\nu=0} \qquad (9)$$

$$(b_3)_{\nu=0} = \left(\frac{4\varepsilon\sigma^{12}}{k_BT}\right)^{0.5}\sum_{t=0}^{11}G_ty_t \qquad (10)$$

$$\left(\frac{\partial b_3}{\partial \nu}\right)_{\nu=0} = -\frac{1}{k_BT}\left(\frac{k_BT}{4\varepsilon\sigma^{12}}\right)^{\frac{1}{4}}\sum_{t=0}^{11}H_ty_t \qquad (11)$$

$$y = 2\left(\frac{\varepsilon}{k_B T}\right)^{\frac{1}{2}}, \qquad G_t = 4\pi^2 \int_0^1 \int_{1-\zeta}^1 C_t \zeta \eta \, d\eta \, d\zeta \tag{12}$$

$$C_t = \tfrac{1}{12}[\zeta^{-6} \ln \zeta^{-12} + \eta^{-6} \ln \eta^{-12} - \langle 6 \rangle \ln \langle 12 \rangle] \tag{13}$$

$$H_t = \frac{\pi^2}{3t!}\Gamma\left(\frac{2t+1}{4}\right) \times \int_0^1 \int_{1-\zeta}^1 \langle 6 \rangle^t \langle 12 \rangle^{-(2t+1)/4} \frac{3\cos\vartheta_1 \cos\vartheta_2 \cos\vartheta_3 + 1}{\eta^2 \zeta^2} \, d\eta \, d\zeta \tag{14}$$

where the pointed brackets symbolize $\langle \alpha \rangle = 1 + \zeta^{-\alpha} + \eta^{-\alpha}$.

In Eq. (8), the coefficients G_t [Eq. (9)] and H_t [Eq. (10)] are as presented in the literature.[1]

Utilizing the grand canonical theory for computing the thermodynamic functions of the state yields the following.[4–8]

Entropy:

$$S = -\left(\frac{\partial \Omega}{\partial T}\right)_{V,\mu} \tag{15}$$

Pressure:

$$p_p = -\left(\frac{\partial \Omega}{\partial V}\right)_{T,\mu} \tag{16}$$

Number of particles:

$$N = -\left(\frac{\partial \Omega}{\partial \mu}\right)_{T,V} \tag{17}$$

Internal energy:

$$U = TS - p_p V + \mu N \tag{18}$$

Free energy:

$$A = -p_p V + \mu N \tag{19}$$

Enthalpy:

$$H = U + p_p V \tag{20}$$

Using Eqs. (19) and (20), we can calculate and express with the free energy some derived thermodynamic properties of state, which are very important in planning and monitoring engineering processes:

$$C_P = \left(\frac{\partial H}{\partial T}\right)_{p_p} = -\left(\frac{\partial A}{\partial T}\right)_V - T\left(\frac{\partial^2 A}{\partial T^2}\right)_V - V\left[\frac{\partial}{\partial T}\left(\frac{\partial A}{\partial V}\right)_T\right]_V \tag{21}$$

The propagation of sonic waves for real fluids is, in most cases, nearly isentropic. Therefore, we can calculate the isentropic speed of sound for a real fluid c_0:

$$c_0 = \sqrt{-V^2\left(\frac{\partial p_p}{\partial V}\right)_S \frac{1}{M}} \tag{22}$$

With help of the first and second laws of thermodynamics, we can rewrite the isentropic speed of sound[5,7]:

$$c_0 = \sqrt{-\frac{V^2}{M}\left[\frac{C_P}{T}\left(\frac{\partial T}{\partial V}\right)_{p_p,\psi} \Big/ \left(\frac{\partial V}{\partial T}\right)_{p_p,\psi} - \frac{C_P}{T}\left(\frac{\partial T}{\partial p_p}\right)_{V,\psi}\right]} \tag{23}$$

Therefore, the velocity of sound is a function of the thermodynamic properties of the fluid. It is evident that all thermodynamic properties in Eq. (23) can be expressed in terms of free energy.

Quantum Corrections to the Cluster Integrals

We consider an expansion with respect to h^2 to find general expressions for the cluster integrals. In our expressions, we considered the diffraction effects. The final expressions for cluster coefficients, including quantum corrections, are presented in the form[1]

$$b_k = b_k^{(0)} + \frac{h^2\beta}{(2\pi)^2 4m} b_k^{(1)} + \left(\frac{h^2\beta}{(2\pi)^2 4m}\right)^2 b_k^{(2)} + \cdots \qquad k = 1, 2, 3, \ldots \tag{24}$$

In Eq. (24), $b_k^{(0)}$ is the classical cluster coefficient and $b_k^{(1)}$ and $b_k^{(2)}$ are quantum correction coefficients. The final results for two-molecule clusters are[1]

$$b_2^{(1)} = -\frac{\pi}{18}\left(\frac{\lambda_{LJ}}{k_B T}\right)^{\frac{1}{12}} \sum_{t=0}^{\infty} (36t - 11)\Gamma\left(\frac{6t-1}{12}\right)\frac{y^t}{t!} \tag{25}$$

$$b_2^{(2)} = \frac{\pi}{180}\left(\frac{\lambda_{LJ}}{k_B T}\right)^{-\frac{1}{12}} \times \sum_{t=0}^{\infty} (3024t^2 + 4728t + 767)\Gamma\left(\frac{6t+1}{12}\right)\frac{y^t}{t!} \tag{26}$$

$$b_2^{(3)} = -\frac{\pi}{420}\left(\frac{\lambda_{LJ}}{k_B T}\right)^{-\frac{1}{4}} \sum_{t=0}^{\infty} (53{,}568t^3 + 303{,}216t^2 + 491{,}076t + 180{,}615)\Gamma\left(\frac{2t+1}{4}\right)\frac{y^t}{t!} \tag{27}$$

$$y = \left(\frac{\mu}{k_B T}\right)\left(\frac{k_B T}{\lambda_{LJ}}\right)^{\frac{1}{2}} \tag{28}$$

$$\lambda_{LJ} = 4\varepsilon\sigma^{12} \tag{29}$$

The final results for a three-molecule cluster are[3]

$$b_3 = \left(b_3^{(0)}\right)_{v=0} + v\left(\frac{\partial b_3^{(0)}}{\partial v}\right) + \frac{\hbar^2}{4mk_B T}\left(b_3^{(1)}\right)_{v=0} \tag{30}$$

$$\left(b_3^{(1)}\right)_{v=0} = \left(\frac{\lambda_{LJ}}{k_B T}\right)^{\frac{1}{3}} \sum_{t=0}^{\infty} I_t y^t \tag{31}$$

where the coefficients I_t are presented in the literature.[3]

Use of Quantum Field Theory

The world of particles can be described as the permanent interaction of a multiparticle system with N particles. For an accurate calculation of thermodynamic functions of state, it would be necessary to resolve Schrödinger's equation for many particles. Even though in this case the multiparticle wave equation contains all of the necessary information, a direct analytical solution of Schrödinger's equation proves to be impossible (see Ref. 8). The computational difficulties in multiparticle systems occur because, in such a case, it is impossible to divide Schrödinger's wave functions into N single-particle independent system that can be resolved analytically. Therefore, this problem can be resolved only by using approximate methods. All such procedures are based on the independent particle model, aimed at translating the N-particle system into N single-particle problems.

We used the theory of a weakly coupled highly degenerate quantum fluid at finite temperature.[8] We used the theory of second quantization or quantum theory of a field as well as Green's functions using Feynman diagrams.[8,9] Even in nonrelativistic theory, second quantization greatly simplifies the discussion of many identical systems. The quantum field theory allows a specific approach to the

solution of Schrödinger's equation for the system of many-coupled particles. The preceding method was successfully used in the analysis of the phenomena of superfluidity, superconductivity processes in nuclei and in many other areas.[8,9] We used the formalism of the quantum field theory for the calculation of thermodynamic functions in the region of temperatures and pressures for engineering applications. To this end, we used the Maxwell–Boltzmann distribution (see Ref. 10) and, as a consequence, neglected the impact of quantum effects. The mathematical model depicted is the first attempt of this kind of the use of quantum field theory for the calculation of thermodynamic functions of state in refrigeration.

In quantum field theory, the concept of the second quantization denotes the creation and annihilation of particles.[5] It is found that in the nonrelativistic theory of fields, second quantization simplifies the complex solution of Schrödinger's equation. To compute thermodynamic functions of state using quantum field theory, the model of weakly coupled quantum fluid is used.[9]

Second quantization theory inherently contains the elements of statistics (bosons and fermions), whereas quantum field theory, on the other hand, allows the computation of matrix elements and avoids a direct calculation of multiparticle wave functions and the coordinates of all remaining particles. The expression of all important properties in quantum field theory is in Green's functions, whose solutions, unfortunately, still represent very complex problems. This is why we employed perturbation theory for the computation of Green's functions.

Schrödinger's Equation of First and Second Quantization

The Hamiltonian for a system of N particles is defined by[7]

$$H_H = \sum_{k=1}^{N} T_k(x_k) + \frac{1}{2} \sum_{k \neq t=1}^{N} V_p(x_k, x_t) \tag{32}$$

In Eq. (32), V_p denotes the interaction between each pair of particles. The variable x_k represents the coordinates of the kth particle, including the space coordinates $\boldsymbol{x}_k$ and discrete variables, such as the spin component. By the use of the Hamiltonian, the time-dependent Schrödinger equation can be written as (see Ref. 8)

$$H_H \psi(x_1, x_2, \ldots, x_N, \tau) = i\hbar \frac{\partial}{\partial \tau} \psi(x_1, x_2, \ldots, x_N, \tau) \tag{33}$$

In Eq. (33), $\psi(x_1, x_2, \ldots, x_N, t)$ represents the many-particle wave function.[10] In physics, the formalism of first and second quantization is frequently used for systems of many particles. The first quantization is a procedure through which quantum-mechanical functions are obtained from classical physical functions. Schrödinger's equation [Eq. (33)] using the first quantization can be written as follows[10,11]:

$$\hat{H}_H |\psi\rangle = i\hbar \frac{\partial}{\partial \tau} |\psi\rangle \tag{34}$$

Equation (34) denotes an operator equation that applies to vectors $|\psi\rangle$ in Hilbert space. In Eq. (34) and in subsequent equations, the carat denotes an operator.

In the second quantization, operators may be used not only to denote the physical functions, but also the states of N-particle systems. In addition to the formal simplicity of the second quantization, a big advantage of quantum field theory is that the statistics of particles can be integrated into the theory and, at the same time, the theory can be expanded also to systems where the number of particles is not constant. Here, the word statistics denotes something different than statistical mechanics. As a matter of fact, the total wave function of a system of particles is symmetric or antisymmetric with regard to the exchange of the position and spin particle operators.[8–11]

Let us begin with the expansion of the multiparticle ψ in a complete set of time-independent, single-particle wave functions $\psi_{E_k}(x_k)$ (Ref. 8). E_k is a complete set of single-particle quantum numbers. It is convenient to imagine that this infinite set of single-particle quantum numbers is ordered (1, 2, 3, …, k, …, ∞) and that E_K runs over this set of eigenvalues. We can now expand the many-body wave function as follows:

$$\psi(x_1, \ldots, x_n, \tau) = \sum_{E_{k=1}}^{E_N} C(E_1, \ldots, E_k, \tau) \psi_{E_1}(x_1), \ldots, \psi_{E_k}(x_k) \tag{35}$$

This expression is completely general and is simply the expansion of the many-particle wave function in a complete set of states. Because $\psi_E(x)$ are time independent, the entire time dependence of the multiparticle wave function is hidden in coefficients C (Refs. 5 and 8). We substitute Eq. (35) into Schrödinger equation [Eq. (33)] and multiply the expression by $\psi_{E_1}(x_1)^+, \ldots, \psi_{E_N}(x_N)^+$ in turn, which is the product of the adjoint wave function in accordance with the adequate final set of quantum numbers $E_1, \ldots, E_N$. On the left-hand side, this procedure selects the coefficient C corresponding to the given set of quantum numbers. The integration over all appropriate coordinates x_k gives the following equation:

$$\begin{aligned} i\hbar \frac{\partial}{\partial \tau} C(E_1, \ldots, E_N, \tau) &= \sum_{k=1}^{N} \sum_{W} \int \mathrm{d}x_k \psi_{E_k}(x_k)^+ T_{k1}(x_k) \\ &\times \psi_W(x_k) C(E_1, \ldots, E_{k-1}, W E_{k+1}, \ldots, E_N, \tau) \\ &+ \frac{1}{2} \sum_{k \neq r=1}^{N} \sum_{W} \sum_{W'} \int\int \mathrm{d}x_k \, \mathrm{d}x_1 \psi_{E_k}(x_k)^+ \psi_{Er}(x_r)^+ V_p(x_k, x_r) \\ &\times \psi_W(x_k) \psi_{W'}(x_r) C(E_1, \ldots, E_{k-1}, W' E_{k+1}, \ldots, E_N, \tau) \end{aligned} \tag{36}$$

In Eq. (36), V_p contains information on two particles. The quantum numbers of the kth particle range over an infinite set of values denoted by W, whereas the quantum numbers of the rth particle range over an infinite set of values denoted by W′. A detailed explanation of Eq. (36) may be found in the literature.[8–10]

Now we substitute the statistics of particles into Eq. (36). The multiparticle wave function can be written as follows[5]:

$$\psi(\ldots, x_i, \ldots, x_j, \ldots, \tau) = \pm \psi(\ldots, x_j, \ldots, x_i, \ldots, \tau) \tag{37}$$

Equation (37) specifies that the wave function can be symmetrical or antisymmetrical if the coordinates of two particles are exchanged. An indispensable and satisfactory condition is that the quantum numbers C correspond to the equation

$$C(\ldots, E_i, \ldots, E_j, \ldots, \tau) = \pm C(\ldots, E_j, \ldots, E_i, \ldots, \tau) \tag{38}$$

Particles that satisfy the positive sign are called bosons, and particles that satisfy the negative sign are called fermions. Sometimes it is useful to employ linear combinations of creation and annihilation operators c and c^+:

$$\hat{\psi}(\boldsymbol{x}) = \sum_k \psi_k(\boldsymbol{x}) c_k, \qquad \hat{\psi}^+(\boldsymbol{x}) = \sum_k \psi_k(\boldsymbol{x}) c_k^+ \tag{39}$$

Such operators $\hat{\psi}$ are called field operators in Hilbert space. In this way, we are able to form appropriate creation and annihilation field operators. In Eq. (39), coefficients c_k are single-particle wave functions and the summation ranges over a total set of single-particle quantum numbers $k = 1, \ldots, N$. Using field operators, we can write the operator $\hat{H}$ (Refs. 2 and 3):

$$\begin{aligned} \hat{H}_H &= \int \mathrm{d}^3 x \hat{\psi}^+(\boldsymbol{x}) T_k(\boldsymbol{x}) \hat{\psi}(\boldsymbol{x}) \\ &+ \frac{1}{2} \int\int \mathrm{d}^3 x \, \mathrm{d}^3 x' \hat{\psi}^+(\boldsymbol{x}) \hat{\psi}^+(\boldsymbol{x}') V_p(\boldsymbol{x}, \boldsymbol{x}') \hat{\psi}(\boldsymbol{x}) \hat{\psi}(\boldsymbol{x}') \end{aligned} \tag{40}$$

This type of expression for the Hamiltonian operator is called the second quantization.

Dyson's Equation

By the use of the perturbation expansion of Green's functions and Dyson's equation, the equation for the calculation of the thermodynamic potential Ω can be written as follows[8]:

$$\Omega(T, V, \mu) = \Omega_0(T, V, \mu) \mp \frac{V}{(2\pi)^3} \int_0^1 \frac{\mathrm{d}\lambda}{\lambda} \int \mathrm{d}^3k \frac{1}{\beta\hbar} \times \sum [\exp(i\omega_n \eta_c)\hbar] \sum^{*\lambda} (\boldsymbol{k}, \omega_n) G^{\lambda}(\boldsymbol{k}, \omega_n) \tag{41}$$

$$\sum^{*} (\boldsymbol{k}, \omega_n)$$

is called the proper self-energy, $G(\boldsymbol{k}, \omega_n)$ is Green's function, λ is the integrational variable, and Ω_0 is the thermodynamic potential for an ideal gas. Equation (41) is the final goal of the use of quantum field theory. The upper (lower) sign ($\mp$) refers to bosons (fermions). Ω may be calculated through the computation of individual proper self-energies and Green's functions. Proper self-energies and Green's functions are the appropriate functions for an interaction potential, and the spin sum gives rise to an added factor of two. The present theory applies to fermions at any temperature and to bosons above the temperature of transition to the original state. The discrete variable

$$\omega_n = \left\{ \begin{array}{ll} \dfrac{2\pi n}{\beta\hbar} & \text{boson} \\ \dfrac{(2n+1)\pi}{\beta\hbar} & \text{fermion} \end{array} \right\} \tag{42}$$

The expression

$$\sum_n \exp(i\omega_n \eta)$$

in Eq. (41) is the frequency sum (see Fig. 1). For the intermolecular potential, we used a new two-Yukawa (TY) function (see Ref. 12). This function is found to mimic very closely the Lennard–Jones (LJ) potential[12] in the region where attraction forces dominate (real gas):

$$V_p(r) = (-k_0\varepsilon\{\exp[-z_1(r-\sigma)]/r\} + k_0\varepsilon\{\exp[-z_2(r-\sigma)]/r\} \quad r > D) \tag{43}$$

where $k_0 = 2.1714\sigma$, $z_1 = 2.9637/\sigma$, and $z_2 = 14.0167/\sigma$. D is defined as[12]

$$D = 2^{\frac{1}{6}} \left[1 + \left(1 + T^* + c_2 T^{*2} + c_3 T^{*4} \right) / c_1 \right)^{\frac{1}{2}} \Big]^{-\frac{1}{6}} \sigma \tag{44}$$

where $c_1 = 1.1287$, $c_2 = -0.05536$, $c_3 = 0.0007278$, and $T^* = k_B T/\varepsilon$. The TY function and the LJ potential are given in Ref. 12, in which practically no differences can be observed in comparison with the LJ potential.

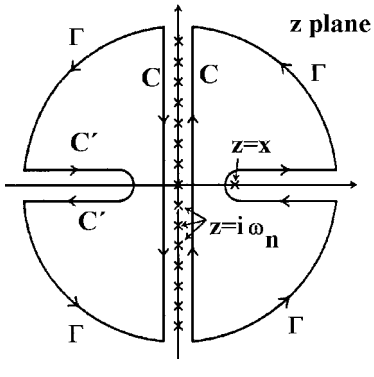

Fig. 1 Contour in frequency sum estimation.

With the help of a Fourier transformation, we can write the TY potential in momentum space[10]:

$$V_p(\boldsymbol{k}) = \int V_p(\boldsymbol{x}) \exp(-i\boldsymbol{k} \cdot \boldsymbol{x})\, \mathrm{d}^3x = 4\pi \int V_p(r) \frac{\sin(kr)}{k} r\, \mathrm{d}r \tag{45}$$

When we introduce Eq. (43) into Eq. (45), we obtain

$$V_p(k) = \frac{4\pi k_0 \varepsilon}{k} \left[\frac{k\cos(k\sigma) + z_2 \sin(k\sigma)}{z_2^2 + k^2} - \frac{k\cos(k\sigma) + z_1 \sin(k\sigma)}{z_1^2 + k^2} \right] \tag{46}$$

The first-order proper self-energy in momentum space is given by Fetter and Walecka[8]:

$$\sum_{(1)}^{*} = \hbar^{-1} \left[(2s_p + 1) V_p(0) (2\pi)^{-3} \int \mathrm{d}^3k n_k \pm (2\pi)^{-3} \int \mathrm{d}^3q n_q V_p(\boldsymbol{k} - \boldsymbol{q}) \right] \tag{47}$$

Molecular distribution is defined as

$$n_k = 1/\exp[(e_k - \mu)/k_B T] \mp 1 \tag{48}$$

where the upper (lower) sign refers to bosons (fermions). We consider the behavior at high temperature and low density, when the quantum-mechanical Fermi–Dirac and Bose–Einstein distribution may be approximated by the classical Boltzmann distribution (see Ref. 5):

$$n_k = 1/\exp[(e_k - \mu)/k_B T] \tag{49}$$

With the help of Feynman's rules,[8] we can express some of the first- and second-order contributions to the proper self-energy. The corresponding first-order term in the thermodynamic potential is given by

$$\Omega_1(T, V, \mu) = \frac{V}{(2\pi)^6} \int \mathrm{d}^3k n_k \left[(2s+1) V_p(0) \int n_q\, \mathrm{d}^3q \pm \int n_q V_p(\boldsymbol{k} - \boldsymbol{q})\, \mathrm{d}^3q \right] \tag{50}$$

where the λ integration has already been performed [see Eq. (41)].

Wick's theorem (see Refs. 8–10) allows us to evaluate the exact Green's function as an exact perturbation expansion involving only field operators in the interaction picture. In that case, the perturbation expansion could be greatly simplified with Wick's theorem, which provided a prescription for relating a T_{k1} product of operators to the normal-ordered product of the same operators. Figure 2 features the first-order contribution to the proper self-energy. Figure 2 in momentum space is called, in quantum field theory, a Feynman diagram because the first diagrammatic expansion of this form was developed by Feynman. A detailed explanation of Feynman's rules for drawing Feynman diagrams is presented in the literature of Fetter and Walecka.[8]

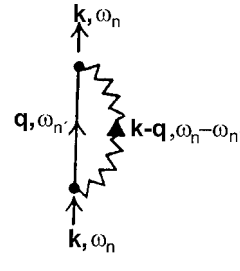

Fig. 2 First-order nontedpole contribution to the proper self-energy.

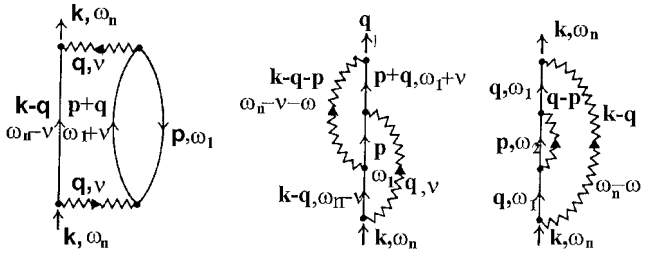

Fig. 3 Second-order nontedpole contributions to the proper self-energy.

It has been shown by the work of Itzykisson and Zuber,[11] Abrikosov et al.,[9] and Fetter and Wallecka,[8] that the terms in Eq. (50) have very little influence at higher temperatures ($T \gg 0$ K). The contributions of second order, shown in Fig. 3, can be expressed by the following equations:

$$\sum_{(2)}^{*}(\boldsymbol{k}, \omega_n) = \pm(-\hbar)^{-2}(-2)(\beta\hbar)^{-2} \times \sum_{\omega_1}\sum_{\nu}(2\pi)^{-6}\int \mathrm{d}^3 p\, \mathrm{d}^3 q[V_p(\boldsymbol{q})]^2 \times G^0(\boldsymbol{p}, \omega_1)G^0(\boldsymbol{q}+\boldsymbol{p}, \omega_1+\nu)G^0(\boldsymbol{k}-\boldsymbol{q}, \omega_1-\nu) \tag{51}$$

$$\sum_{(2)}^{*}(\boldsymbol{k}, \omega_n) = \pm(-\hbar)^{-2}(\beta\hbar)^{-2}\sum_{\omega_1}\sum_{\nu}(2\pi)^{-6} \times \int \mathrm{d}^3 p\, \mathrm{d}^3 q[V_p(\boldsymbol{q})V_p(\boldsymbol{k}-\boldsymbol{q}-\boldsymbol{p})]G^0(\boldsymbol{k}-\boldsymbol{q}, \omega_n-\nu) \times G^0(\boldsymbol{p}, \omega_1)G^0(\boldsymbol{p}+\boldsymbol{q}, \omega_1+\nu)G^0(\boldsymbol{p}+\boldsymbol{q}, \omega_1+\nu) \tag{52}$$

$$\sum_{(2)}^{*}(\boldsymbol{k}, \omega_n) = \pm(-\hbar)^{-2}(\beta\hbar)^{-2}\sum_{\omega_1\omega_2}(2\pi)^{-6} \times \int \mathrm{d}^3 p\, \mathrm{d}^3 q[V_p(\boldsymbol{k}-\boldsymbol{q})V_p(\boldsymbol{q}-\boldsymbol{p})] \times G^0(\boldsymbol{q}, \omega_1)G^0(\boldsymbol{p}, \omega_2)\exp(i\omega_2\eta)G^0(\boldsymbol{q}, \omega_1) \tag{53}$$

The analytical computation of second-order terms is extremely demanding in the case of complex potentials. In the practical engineering temperature domain ($T \gg 0$), however, the values of second and higher-order terms are also negligible, except for Feynman's graph, shown in Fig. 4, where his ring diagram is presented. The source of the divergence in second- and higher-order terms of ring diagrams is the occurrence of the same momentum transfer, $hq/2\pi$ (Fig. 4), on each interaction line.

The fundamental approximation in quantum field theory is to retain this selected class of most divergent higher-order diagrams along with the complete first- and second-order contributions

$$\sum^{*} = \sum_{(1)}^{*} + \sum_{n=2}^{\infty}\sum_{(n)r}^{*} \tag{54}$$

$$\sum^{*} = \sum_{(1)}^{*} + \sum_{r}^{*} \tag{55}$$

where

$$\sum_{r}^{*}$$

is the sum of all self-energy diagrams with the construction of Fig. 4.

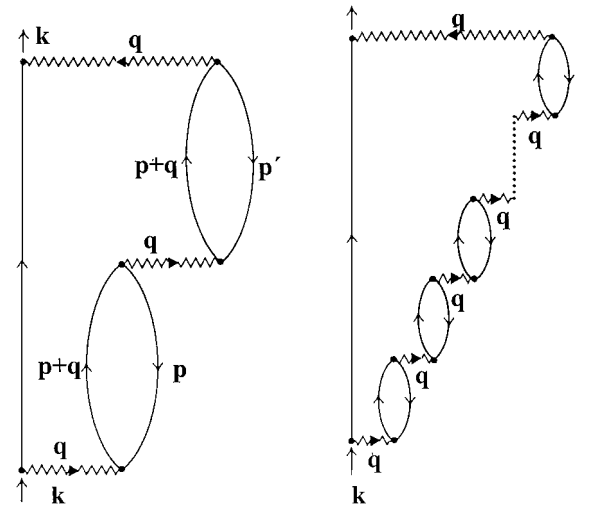

Fig. 4 Ring contribution to the proper self-energy in third- and higher-order terms.

In the classical limit (Maxwell–Boltzmann distribution) we can express the dominant contribution Ω_R as

$$\Omega_R = \frac{1}{2}Vk_BT(2\pi)^{-3}\int \mathrm{d}^3 q\left\{\ell n\left[1 - V_p(q)2\beta\exp(\beta\mu)\lambda_T^{-3}\varphi(q\lambda_T)\right] + V_p(q)2\beta\exp(\beta\mu)\lambda_T^{-3}\varphi(q\lambda_T)\right\} \tag{56}$$

$$\varphi(x) = \frac{1}{\pi x}\int_0^{\infty}\xi\,\mathrm{d}\xi\exp\left(-\frac{\xi^2}{4\pi}\right)\ell n\left|\frac{2\xi+x}{2\xi-x}\right| \tag{57}$$

We can insert the TY potential expressed in momentum space [Eq. (46)] in Eq. (56), and integrating by parts gives

$$\Omega_R = -\frac{1}{2}Vk_BT(2\pi)^{-3}4\pi \times \int_0^{\infty}\frac{k^3}{3}\left[2\beta\exp(\beta\mu)\lambda_T^{-3}4\pi k_0\varepsilon\right]^2\frac{1}{1+P}\left(\frac{K_1+K_2+K_3}{k^3} + \frac{K_4+K_5+K_6+K_7+K_8+K_9+K_{10}+K_{11}}{k^2}\right)\mathrm{d}k \tag{58}$$

$$P = 2\beta\exp(\beta\mu)\lambda_T^{-3}\frac{4\pi k_0\varepsilon}{k} \times \left[\frac{k\cos(k\sigma)+z_2\sin(k\sigma)}{z_2^2+k^2} - \frac{k\cos(k\sigma)+z_1\sin(k\sigma)}{z_1^2+k^2}\right] \tag{59}$$

Equation (58) shows the integral, whereas individual functions K_i, needed in the integration, are indicated in Table 1. The analytical solution of the integral in Eq. (58) is a difficult task. Reasonably accurate results can be obtained by means of generalizations induced by fast convergence of the coefficient P:

$$\Omega_R = -\frac{1}{2}Vk_BT(2\pi)^{-3}4\pi\int_0^{\infty}\frac{k^3}{3}\left(2\beta\exp(\beta\mu)\lambda_T^{-3}4\pi k_0\varepsilon\right)^2 \times \left[\frac{K_1+K_2+K_3}{k^3} + \frac{\sum_4^{11}K_i}{k^2}\right]\mathrm{d}k \tag{60}$$

The analytical solution of Eq. (60) is expressed by the following equation:

$$\Omega_R = \tfrac{1}{2}Vk_BT(2\pi)^{-3}\left[2\beta\exp(\beta\mu)\lambda_T^{-3}4\pi k_0 es^2\right]^2 4\pi\sigma K_K \tag{61}$$

These findings were used to calculate the integral in Eq. (60). The analytical expressions for the integrals in Eq. (61) are presented in literature.[13] The set of 23 coefficients is hidden in the constant K_K. It is possible to calculate K_K analytically. In our case, we determined the coefficients by comparison between experimental data and analytical results. For methane, we determined that K_K is 0.001. With the help of Eq. (61), we can calculate all important thermodynamic functions [see Eqs. (41) and (15–20)].

Table 1 Terms of thermodynamic potential Ω_R

i	K_i
1	$\frac{[k\cos(k\sigma)+z_2\sin(k\sigma)]^2}{\left(z_2^2+k^2\right)^2}$
2	$-2\frac{[k\cos(k\sigma)+z_2\sin(k\sigma)][k\cos(k\sigma)]+z_1\sin(k\sigma)}{\left(z_2^2+k^2\right)\left(z_1^2+k^2\right)}$
3	$+\frac{[k\cos(k\sigma)+z_1\sin(k\sigma)]}{\left(z_1^2+k^2\right)^2}$
4	$-\frac{k\cos(k\sigma)+z_2\sin(k\sigma)}{\left(z_2^2+k^2\right)^2}[\cos(k\sigma)-k\sigma\sin(k\sigma)+z_2\sigma\sin(k\sigma)]$
5	$+\frac{[k\cos(k\sigma)+z_1\sin(k\sigma)]}{\left(z_2^2+k^2\right)\left(z_1^2+k^2\right)}[\cos(k\sigma)-k\sigma\sin(k\sigma)+z_2\sigma\sin(k\sigma)]$
6	$+\frac{[k\cos(k\sigma)+z_2\sin(k\sigma)]}{\left(z_2^2+k^2\right)^3}[k\cos(k\sigma)+z_2\sin(k\sigma)]2k$
7	$-\frac{[k\cos(k\sigma)+z_2\sin(k\sigma)]}{\left(z_1^2+k^2\right)\left(z_2^2+k^2\right)^2}[k\cos(k\sigma)+z_2\sin(k\sigma)]2k$
8	$-\frac{[k\cos(k\sigma)+z_2\sin(k\sigma)]}{\left(z_2^2+k^2\right)\left(z_1^2+k^2\right)}[\cos(k\sigma)-k\sigma\sin(k\sigma)+z_1\sigma\sin(k\sigma)]$
9	$\frac{[k\cos(k\sigma)+z_1\sin(k\sigma)]}{\left(z_1^2+k^2\right)^2}[\cos(k\sigma)-k\sigma\sin(k\sigma)+z_1\sigma\sin(k\sigma)]$
10	$\frac{[k\cos(k\sigma)+z_2\sin(k\sigma)]}{\left(z_2^2+k^2\right)\left(z_1^2+k^2\right)^2}[k\cos(k\sigma)+z_1\sin(k\sigma)]2k$
11	$-\frac{[k\cos(k\sigma)+z_1\sin(k\sigma)]}{\left(z_1^2+k^2\right)^3}[k\cos(k\sigma)+z_1\sin(k\sigma)]2k$

Results and Discussion

We carried out calculations for hydrogen and methane. The comparison of our calculations with thermodynamic data and experimental results by Gammon and Douslin,[14] Zemansky and Dittman,[6] and Younglove and Ely[15] are presented in Tables 2 and 3 and Figs. 5–7.

We compared the models obtained by statistical thermodynamics, statistical theory with the help of the classical virial expansion (ST) [Eqs. (6) and Eq. (7)], statistical theory with the help of virial expansion and quantum corrections (STK) [Eq. (24)], the models obtained by quantum field theory (QFT) (and QFT-TY, weakly coupled quantum fluid based on of the two-Yukawa function) [Eq. (61)], and experimental results. In the procedure of computing the cluster integrals with the help of statistical thermodynamics on the basis of the classical virial expansion (ST) and the virial expansion with quantum corrections, the effects of mutual interactions of up to three molecules in the cluster were taken into account.[5]

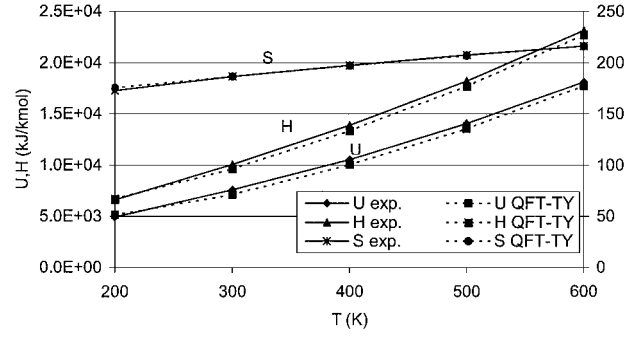

Fig. 5 Comparison between analytical results and experimental data for methane at 1 bar (AAD for $U = 4.2\%$, $H = 2.8\%$, and $S = 0.4\%$).

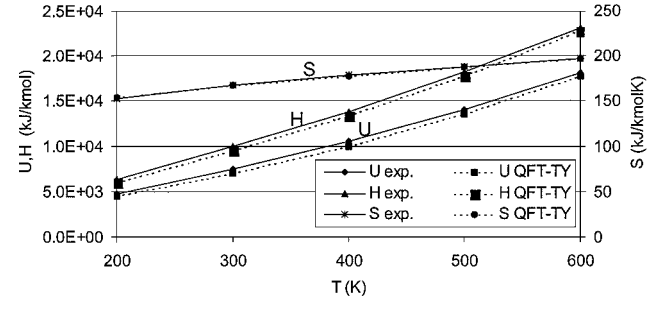

Fig. 6 Comparison between analytical results and experimental data for methane at 10 bar (AAD for $U = 4.1\%$, $H = 3.2\%$, and $S = 0.2\%$).

Table 2 Enthalpy of hydrogen (R702)

	H, kJ/kmol			AD			
Model	$p_p = 1$ bar	$p_p = 10$ bar	$p_p = 20$ bar	$p_p = 1$ bar	$p_p = 10$ bar	$p_p = 20$ bar	AAD
			T = 60 K				
ST	1586	1430	1250	0.0025	0.05298	0.131944	0.06248
STK	1591	1479	1440	0.0006	0.02053	0	0.00705
QFT-TY	1605	1604	1603	0.0094	0.06225	0.113194	0.06162
Experiment	1590	1510	1440	——	——	——	——
			T = 90 K				
ST	2268	2172	2070	0.008	0.01272	0.037209	0.019312
STK	2269	2190	2118	0.0084	0.00454	0.014884	0.009291
QFT-TY	2279	2279	2278	0.0128	0.03590	0.059535	0.036111
Experiment	2250	2200	2150	——	——	——	——
			T = 120 K				
ST	3054	2998	2937	0.0458	0.03379	0.016263	0.031982
STK	3055	3004	2951	0.0154	0.03586	0.021107	0.024127
QFT-TY	3061	3061	3061	0.0482	0.05551	0.05917	0.054325
Experiment	2920	2900	2890	——	——	——	——

Table 3 Influence of quantum corrections at low temperature for methane

Parameter	Experiment	ST	STK
	$T = 113.1$ K, $V = 7.905$ m^3/kmol		
c_0, m/s	272.83	274.7	273.6
C_v/R_m	3.081	3.02	3.04
p_p, bar	1.1288	1.154	1.134
	$T = 133.1$ K, $V = 2.251$ m^3/kmol		
c_0, m/s	284.6	288.8	288.2
C_v/R_m	3.178	3.095	3.11
p_p, bar	4.36	4.53	4.53
	$T = 153.1$ K, $V = 0.85$ m^3/kmol		
c_0, m/s	285.7	294	293.9
C_v/R_m	3.354	3.187	3.190
p_p, bar	11.8	12.57	12.6

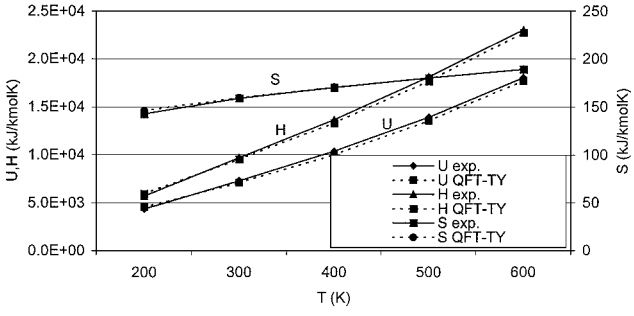

Fig. 7 Comparison between analytical results and experimental data for methane at 25 bar (AAD for U = 3.1%, H = 0.6%, and S = 0.6%).

Table 2 shows the deviation of the analytical computation of enthalpy for hydrogen for the real-gas region from the experimental values. The results obtained by the virial expansion with the help of quantum corrections (STK) show good agreement. The theory of virial expansion with the help of quantum corrections yields worse results than the STK model, especially at low temperatures and higher pressures. Somewhat larger deviations, especially at high pressures, are observed from using QFT due to the poorer approximation of attractive forces and the domination of repulsive forces in the region where repulsive forces dominate. The maximum absolute deviation (AD) was ST 13.1%, QFT-TY 11.1%, and STK 3.5% for temperatures between 60 and 120 K and for pressures between 1 and 20 bar.

Table 3 shows the deviation of the analytical results obtained with statistical thermodynamics (ST, STK) for methane in comparison with experimental data. It is possible to calculate the isochoric molar capacity with the help of the following expression:

$$C_V = \left(\frac{\partial U}{\partial T}\right)_V \tag{62}$$

The computed pressure, molar heat at constant volume, and velocity of sound conform well to the measured results.

Figures 5, 6, and 7 are presentations of entropy, enthalpy, and internal energy for methane. These results were obtained using the QFT-TY. Figures 5–7 also show a comparison between the experimental results for the range between 1 and 25 bar and the temperature range of 200–600 K. Examination of the results indicates that the analytical values are in good agreement with the experimental data. In the higher pressure range (over 25 bar), a tendency is observed toward a substantial increase in the absolute average deviation (AAD) over 5%. The AAD shows (see Figs. 5–7 and Table 2) that QFT-TY gives surprisingly good results in comparison with experimental data.

Conclusions

The paper presents the mathematical model for the computation of thermodynamic functions of the state in the gaseous region at higher temperatures and pressures. We used statistical thermodynamics theory based on the LJ potential.

For the real-gas region, we developed a model with help of QFT. This model is the first attempt for calculating the thermodynamic functions of refrigerants at temperatures $T \gg 0$ K. The analytical results obtained by statistical thermodynamics were compared with thermodynamic data. The results show relatively good agreement.

The computed thermodynamic properties in the real-gas region conform well in comparison with thermodynamic data. The best results are obtained with the model based on statistical thermodynamics and quantum corrections.

In our further research, we intend to extend the presented mathematical model to the calculation of mixtures and to include the theory of fluctuation, which is of great importance in the vicinity of the critical point.

References

[1] Kihara, T., *Intermolecular Forces*, Wiley Chichester, New York, 1976, pp. 17–97.

[2] Lucas, K., *Applied Statistical Thermodynamics*, Springer-Verlag, New York, 1992, pp. 27–141.

[3] Barker, J. A., and Henderson, D., "What Is Liquid," *Reviews of Modern Physics*, Vol. 48, No. 3, 1976, pp. 587–671.

[4] Smirnova, N. A., *Methods of the Statistical Thermodynamics in Physical Chemistry*, Univ. of Moscow, Moscow, 1982, pp. 320–430.

[5] Reichl, L. E., *A Modern Course in Statistical Physics*, University of Texas Press, Austin, TX, 1982, pp. 399–453.

[6] Zemansky, M. W., and Dittman, R. H., *Heat and Thermodynamics*, McGraw–Hill, New York, 1997, pp. 84–175.

[7] Guggenheim, E. A., *Thermodynamics, An Advanced Treatment for Chemists and Physics*, North-Holland, Amsterdam, 1993, pp. 82–169.

[8] Fetter, A. L., and Walecka, J. D., *Quantum Theory of Many-Particle Systems*, McGraw–Hill, New York, 1976, pp. 227–290.

[9] Abrikosov, A. A., Gorkov, L. P., and Dzayaloshinski, I. E., *Methods of Quantum Field Theory in Statistical Physics*, Prentice–Hall, Englewood Cliffs, NJ, 1963, pp. 85–144.

[10] Merzbacher, E., *Quantum Mechanics*, Wiley, Tokyo, 1976, pp. 28–251.

[11] Itzykisson, C., and Zuber, J. P., *Quantum Field Theory*, McGraw–Hill, New York, 1987, pp. 12–123.

[12] Tang, Y., and Lu, B. C.-Y., "Analytical Representation of the Radial Distribution Function for Classical Fluids," *Molecular Physics*, Vol. 9, No. 2, 1997, pp. 215–224.

[13] Avsec, J., "Calculating the Thermodynamic Functions of State for Some Important Refrigerants," Ph.D. Dissertation, Dept. of Thermophysics, Univ. of Maribor, Maribor, Slovenia, Sept. 1999, pp. 100–160.

[14] Gammon, B. E., and Douslin, D. R., "The Velocity of Sound and Heat Capacity in Methane from Near-Critical to Subcritical Conditions and Equation-of-State Implications," *Journal of Chemical Physics*, Vol. 64, No. 1, 1976, pp. 203–218.

[15] Younglove, B. A., and Ely, J. F., "Thermophysical Properties of Fluids. II, Methane, Ethane, Propane, Isobutane and Normal Butane," *Journal of Physical Chemistry Reference Data*, Vol. 16, No. 4, 1987, pp. 577–798.